Very massive stars chemical enrichment in extremely metal-poor galaxies

A. Bressan[1], G. Costa[2], S. Goswami[3], V. Grisoni[4], K. G. Shepherd[1], L. Silva[5], F. Addari[1], and P. Marigo[2]

[1] SISSA, Via Bonomea 265, I-34136 Trieste, Italy e-mail: `sbressan@sissa.it`
[2] UNIPD, Padova, Italy
[3] CENTRA, Av. Rovisco Pais 1, 1049-001 Lisboa, Portugal
[4] UNIBO, Bologna, Italy
[5] INAF,OATS, Via Tiepolo 11, I-34131 Trieste, Italy

Abstract. In a recent search for the most metal poor local galaxies, EMPRESS, a peculiar class of objects has been discovered. It consists of a sample of extremely metal-poor starburst galaxies showing Fe/O ratios that, beginning from an almost solar value, rapidly decrease at increasing metallicity; in contrast, their N/O ratios are typical of low metallicity stars. Here we report on our investigations on which early stellar populations could be responsible of such surprising trends. We have calculated new models of rotating very massive stars of Pop III and very low metallicity, up to the beginning of the pair-instability phase, and have obtained new yields of pair instability supernovae. We show that, by adopting these yields and a suitable top-heavy initial mass function, is possible to obtain chemical evolution models that are able to reproduce the observed abundance ratios and the young ages of such galaxies.

1. Introduction

Extremely metal-poor galaxies (EMPGs) are defined to have metallicities less than 12+log(O/H)=7.69 (Izotov et al. 2012; Isobe et al. 2020). They have low stellar masses ($\log(M_\star/M_\odot)$ ~6-9) and high specific star formation rates (sSFR~10-100 Gyr^{-1}) (Izotov & Thuan 1998; Pustilnik et al. 2005; Skillman et al. 2013; Hirschauer et al. 2016; Hsyu et al. 2017). Their nature is of great interest since they are considered as local analogs of high redshift galaxies (Vanzella et al. 2017; Stark et al. 2017). In a recent survey, EMPRESS ("Extremely Metal-Poor Representatives Explored by the Subaru Survey"), Kojima et al. (2020) found that EMPGs show neon- and argon-to-oxygen abundance ratios (Ne/O, Ar/O) similar to those of known local dwarf galaxies and that the nitrogen-to-oxygen abundance ratios (N/O) are lower than 20% of the solar N/O value, in agreement with the low oxygen abundance. The iron-to-oxygen (Fe/O) ratios were found to decrease at increasing metallicity, as in the star-forming-sample of

Izotov et al. (2006), but beginning with two representative EMPGs with exceptionally high Fe/O values. In Kojima et al. (2020), three scenarios that might explain the observed Fe/O ratios of their EMPGs were suggested: i) the preferential dust depletion of iron, ii) a mix of metal enrichment and gas dilution caused by inflow, and iii) the contribution of super massive stars, beyond 300 $M_\odot$. In the first scenario the authors assume that the gas-phase Fe/O abundance ratios of the EMPGs decrease with metallicity, because Fe can be depleted into dust more efficiently than O (Rodríguez & Rubin 2005; Izotov et al. 2006); this depletion becomes important at higher metallicities, where dust is produced more efficiently. However, Kojima et al. (2020) did not find evidence that galaxies with a larger metallicity have a larger color excess, i.e. more dust rich. Hence, the Fe/O decrease of their sample seems not due to dust depletion. In their second scenario, it is assumed that these metal-poor galaxies formed from a metal-enriched gas, having already solar metallicity and solar Fe/O value. Then, under a continuous infall of primordial gas, the metallicity (O/H) will decrease, whereas the Fe/O ratio will not change. The almost solar Fe/O ratios, could thus be explained bur one would expect to find almost solar N/O ratios as well. Instead, the two peculiar EMPGs with the higher Fe/O ratios show low N/O ratios (lower than 20% of the solar value), at variance with what would have been expected by this second scenario. Finally, in the third scenario the authors follow the suggestion by Ohkubo et al. (2006), who showed that stars with masses beyond 300 $M_\odot$ can produce large amounts of iron during supernova (SN) explosions. Kojima et al. (2020) suggested that this contribution of iron could produce the high Fe/O ratios observed in the two EMPGs. Furthermore, since explosions of super massive stars do not change the relative N and O ejecta, (Iwamoto et al. 1999; Ohkubo et al. 2006), this model could also explain the observed N/O ratios. This latter scenario is quite appealing because very massive stars are indeed predicted to form in a typical Population III (Pop III) environment with primordial composition gas(e.g. Hirano et al. 2014). There is also compelling evidence for such very massive stars, like the very young ages obtained from the spectro-photometric synthesis of the dominant starburst in the whole local EMPG sample(Kojima et al. 2021). Furthermore, Goswami et al. (2021) provided new yields of massive and very massive stars up to 350 $M_\odot$, and tested them against observations of Galactic thin and thick disc stars, finding that the latter component could be better reproduced using ejecta from pair instability SN (PISN). These models possess an early phase with a high Fe/O ratio after which they rapidly evolve into the domain of the α-enhanced (low Fe/O) thick disc stars. Based on these findings, we address here a twofold aim. First, we test whether the high Fe/O abundance ratios of the EMPGs can be reproduced by PISN yields. Second, we investigate the conditions under which the observed fast decrease of the Fe/O ratio, at increasing O/H abundance, could be obtained in galaxies that otherwise have similar low masses and similar high sSFR. In doing so, we keep in mind that the models must also reproduce the observations of the N/O ratios. To do this, we make use of chemical evolution models that include new stellar yields from our rotating very massive stars, that are briefly discussed in the next section.

2. Chemical evolution with rotating very massive stars

Goswami et al. (2021) calculated chemical yields of non rotating low metallicity very massive stars models computed with PARSEC (Bressan et al. 2012; Chen et al. 2015). While these stars may be important producers of Fe, their contribution to N abundances are negligible. On the contrary, rotating massive stars show significant N production (Meynet et al. 2006; Limongi & Chieffi 2018) during their pre-supernova evolution and, if they explode as PISN, they can also contribute to both O and Fe Takahashi et al. (2018). To better highlight the sensitivity of N production to varying rotational velocity and initial metallicity, we show in Figure 1, the pre-PISN evolution
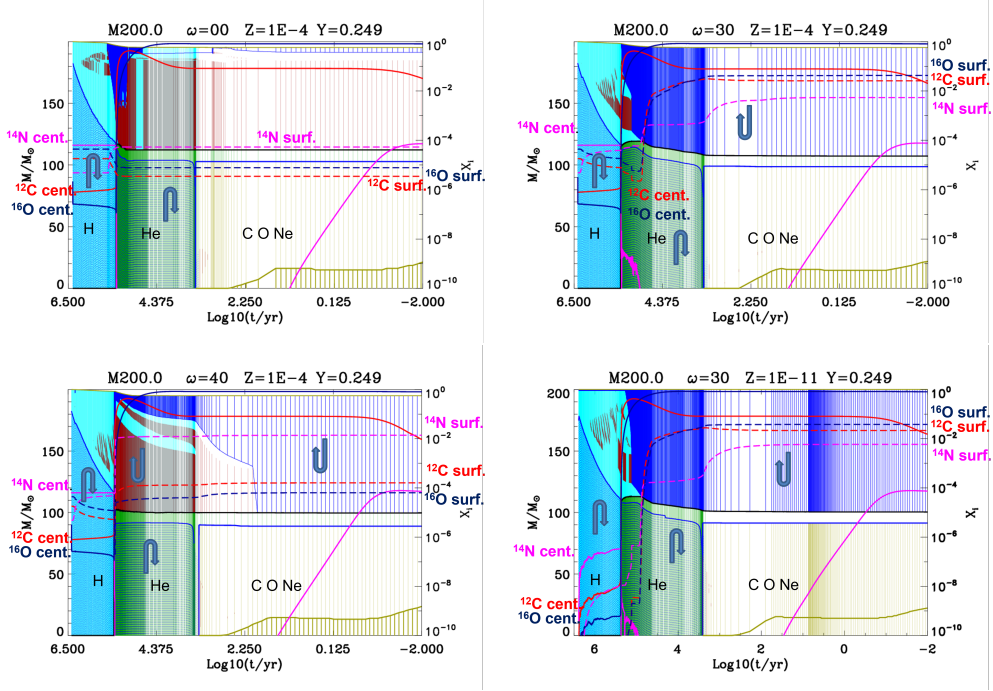
Fig. 1. CNO evolution in 200 $M_\odot$ massive star models at very low metallicity. Surface (central) abundances are indicated by red, magenta and dark-blue dashed (solid) lines, respectively. The abscissa is time from the beginning of the PISN instability ($\Gamma_1 \leq 4/3$) and the ordinate is interior mass in solar masses. ω represents the ratio between initial and critical angular velocities. Convective zones (CZ) are indicated by turn-up (envelopes) and turn-down (cores) arrows; brown hatched regions are intermediate CZ.

of new Pop III models for a star of 200 $M_\odot$, computed with PARSEC (Costa et al. 2022, in preparation). We easily deduce from the figure that i) the model without rotation shows negligible "new" surface N production; ii) N production increases with rotation; iii) for the same initial rotation rate, the new N production is almost independent from the initial metallicity, at least for $Z_i \leq 0.0004$. More details on the new PARSEC models of massive and rotating stars stars can be found in Volpato et al. (2022); Costa et al. (2021); Nguyen et al. (2022). We now define the possible chemical evolution models on the basis of the the chemical properties shown by EMPGs, in particular EMPG 3 and EMPG 10, in Figure 2. They posses (i) a relatively high 12+log(O/H) at very young ages, (ii) high Fe/O ratios and (iii) "standard", i.e. typical of low metallicity stars, N/O ratios. The first point indicates a rapid and efficient enrichment. For this purpose we adopt chemical evolution models with star formation efficiency $\nu = 1$ Gyr^{-1} and $t_{inf} = 0.1$ Gyr (Table 1). The second point might be obtained only by means of a suitable population of PISN with Fe-reach yields, i.e. with initial masses as high as $M_i = 200\ M_\odot - 300\ M_\odot$. Then we adopt a bimodal IMF with an early phase IMF of the form:

$$\frac{dn}{d\log(M_i)} \propto M_i^{-1.3} \times exp\left[-\left(\frac{M_{char}}{M_i}\right)^{1.6}\right] . \ (1)$$

This distribution has already been adopted by Wise et al. (2012) to sample the IMF of Pop III stars, with characteristic masses around $M_{char} = 40\ M_\odot$. Goswami et al. (2022) tested a mass distribution of rotating stars with M_i between 80 $M_\odot$ and 350 $M_\odot$ and with $M_{char} = 200\ M_\odot$ or $M_{char} = 300\ M_\odot$, to maximize Fe production

by the corresponding PISNs (Woosley et al. 2002). These distributions produce almost the same results while, for $M_{char} < 200\ M_\odot$, Fe production would be too small.

We also assume that the early phase of very massive object (VMO) formation continues until the gas metallicity reaches a threshold metallicity defined as $Z_{cr}= Z/Z_\odot$. For metallicities larger than Z_{cr}, we adopt a Kroupa-like IMF, with an exponent x_{UP}=1.3 and upper mass limit M_{UP}=40 $M_\odot$, so that VMOs are no longer produced. We adopt here $Z_{cr} = 10^{-4}$, which is in the range suggested by Salvadori et al. (2008). The third point requires models with initial rotation parameters $\omega=\Omega/\Omega_{crit}$=0.3 and 0.4, as shown by (Goswami et al. 2022) who already calculated yields of very massive stars models of Costa et al. (2022, in preparation). We note that, since we use explosive yields from (Woosley et al. 2002), the range of PISN masses is determined by the He core mass in the latter models, i.e. 65 $M_\odot \leq M_{He} \leq 130\ M_\odot$. The relation with the initial mass depends, beside rotation (Yoon et al. 2012), on the metallicity, mass-loss rate, nuclear reactions and convective overshooting (Costa et al. 2021). The other parameters of the chemical evolution models are reported in Table 1. All the models begin from a metal free gas, $Z=10^{-10}$. Model M13 is computed with yields obtained with PISN models with rotation parameter ω=0.3, while model M14 is computed for a larger rotational velocity ω=0.4. Their metallicity remains flat until the first PISN explosion, after about ~2.3 Myr. This is the typical lifetime of a very massive massive Pop III star. After this age, with the adopted chemical evolution parameters, the metallicity rises very fast. Model M14 reaches Z_{cr}= 0.0001 almost immediately, challenging further formation of VMOs. However, during the first 2.3 Myr, about 180 VMO stars have already been formed, out of the total accumulated stellar mass of about M_{acc}= 38000 $M_\odot$. The models metallicity reaches Z_{cr} at an age of $t_{Z_{cr}}$ ~2.8 Myr. At this point, the IMF turns to a Kroupa-like IMF with un upper mass limit of M_i= 40 $M_\odot$. However, the metallicity enrichment from the VMO burst is effective until an age of $t_{Z_{cr}}$ + 2.3 Myr is reached. Thus

the metal enrichment continues up to about 5 Myr and, after this age, further metal enrichment is only due to massive stars with $M_i \leq 40\ M_\odot$. The value of the O abundance reached at Z_{cr}=0.0001, shown in Column 4 of Table 1, is 12+log(O/H)~ 4.5, i.e. about two orders of magnitude less than that observed in EMPG 3 and EMPG 10. However, further enrichment by the youngest VMOs pushes the value of 12+log(O/H) up to that observed in EMPG 3 and EMPG 10, at an age of about 5 Myr (see also Figure 2). After this age, the metallicity shows a slight decrease until the enrichment by less massive stars begins to compensate for the dilution due to infalling gas. During this phase, 12+log(O/H) decreases by 0.4 dex. The total number of VMO stars formed during the early evolution of the starburst up to Z_{cr}, N_{VMO}, is indicated in the last three columns of Table 1. The third to last column refers to the adopted models, while the last two columns refer to the numbers of VMOs expected from models whose total stellar mass equals the observed galaxy stellar masses, at the corresponding values of 12+log(O/H). The evolution of Model M13 is very similar to that of Model M14. The evolution of the Fe/O and N/O ratios of the models is also shown in Figure 2. Models with an initial rotation parameter ω=0.3 are shown by solid black lines while those with ω=0.4 by dashed black lines. In all plots, the solid black squares along the models mark ages of 5, 20, 30, 60, 100, 200 Myr, with the latter being the rightmost point. In the Fe/O vs O/H diagram the models run almost superimposed and objects EMPG 3 and EMPG 10 can be well fitted for any rotation value. This is because Fe and O are mainly produced during the explosive phase and have much less direct dependence on the initial angular rotation rate than e.g. N. The time-scale of enrichment indicates, at least for EMPG 10, an age slightly larger than 5 Myr, which is compatible with the very young ages derived from spectro-photometry (Kojima et al. 2021). EMPG 3 could also be compatible with an even lower Fe/O ratio with an age that, in this case, would be in better agreement with the quoted one. The N/O ratio of EMPG 10 is marginally fit with the higher rotation young model. For EMPG 3 we

Table 1. Chemical evolution parameters and properties of the VMO burst at $Z=Z_{cr}$.

M_{char} = 200 $M_\odot$	Z_{cr} = Z/Z$_\odot$=1E-4		k=1	τ_{inf} = 0.1		A_{SNIa}=0.04	
Name	ν	ω	t$_{Z_{cr}}$	12+log(O/H)	$Macc$	N$_{VMO}$	
	Gyr^{-1}		Myr		$M_\odot$	Model	EMPG3[a]	EMPG10[a]
M13	1	0.3	2.77	4.520	3.814E4	176	194	393
M14	1	0.4	2.78	4.580	3.834E4	177	194	394
M53	5	0.3	2.70	4.692	3.615E5	1672	2122	4526
M54	5	0.4	2.70	4.663	3.596E5	1675	2100	4454

[a]After re-normalization to the observed stellar mass at the corresponding value of 12+log(O/H).

have only an upper limit on the N/O ratio, and model M14 fits its position very well in both Fe/O and N/O diagrams. However, this model might require two quite different ages for Fe/O and N/O abundance ratios, respectively. The best solution, for Z_{cr} = 0.0001, is provided by model M14 with an age ≥ 30 Myr. Beside reproducing the observed high Fe/O and normal N/O ratios of EMPG 3 and 10, models M13 and M14 show also another interesting feature: their Fe/O rapidly declines at increasing 12+log(O/H), as a consequence of the suppression of the VMO formation when they reach the critical metallicity. However the suppression of the VMO to PISN channel may also be due to stellar evolution itself when, above a critical metallicity, Z_{crse} large mass-loss rates are boosted, challenging the growth of the He core mass (Kozyreva et al. 2014). In our models and for an M_{UP} =350 $M_\odot$, the critical metallicity due to stellar evolution is Z_{crse} ~0.4 (Goswami et al. 2021).

Actually, the EMPGs in Figure 2 are really suggestive of a declining Fe/O ratio at increasing 12+log(O/H). However this trend cannot be explained by the models presented in the upper panels, if we also consider that the observed EMPGs are dominated by starbursts with ages below 50 Myr. Our oldest models have an age of 200 Myr and marginally reach the bulk of the remaining metal poor galaxies in the upper Fe/O diagram, while they do not reach them in the corresponding N/O diagram. We note, however, that many of such EMPGs show Fe/O and N/O ratios that are even below the bulk of the observed values. While low values of N/O are expected among non-rotating models, the observed low Fe/O ratios

could thus challenge standard chemical evolution models. However, low Fe/O ratio could be also indicative of an excess of O, produced by the less massive PISN (Takahashi et al. 2018). We suggest here that the relatively low Fe/O ratio of "evolved" young metal poor starburst galaxies could be explained by a combination of an early burst of VMO, like the one used for EMPG 3 and EMPG 10, and a population of stars that continues to produce O-rich/Fe-poor ejecta. This model could have the twofold effect of favoring a fast 12+log(O/H) evolution and, at the same time, a rapid decline of the Fe/O ratio. We can obtain such a model by simply combining an early burst of VMO stars, like in the case of models M13, M14 and a model that includes a top-heavy IMF with M_{UP} ≤ 200 $M_\odot$ even above Z_{cr} . To obtain such a model, we adopt for the VMOs component the same form of the M13 IMF but, when Z_{cr} = 0.0001 is reached and the IMF turns into a standard Kroupa-like one, we allow the formation of a small fraction low mass VMOs by assuming M_i ≤ 150 $M_\odot$ and an exponent x_{UP} = 0.9. Furthermore, in order to comply with the fast enrichment required by the age estimates performed by Kojima et al. (2021), we need to use a relatively higher star formation rate efficiency of ν = 5 Gyr^{-1}. The properties of these new models, M53 and M54, are shown in Table 1. The evolution of the Fe/O and N/O ratios obtained with these models is shown in the lower panels of Figure 2. Their metallicity 12+log(O/H) rises rapidly up to the value corresponding to Z_{cr} = 0.0001. Beyond this point, the Fe/O ratios, that initially match those of EMPG 3 and EMPG 10, begin a rapid decrease, reaching the value observed in EMPG
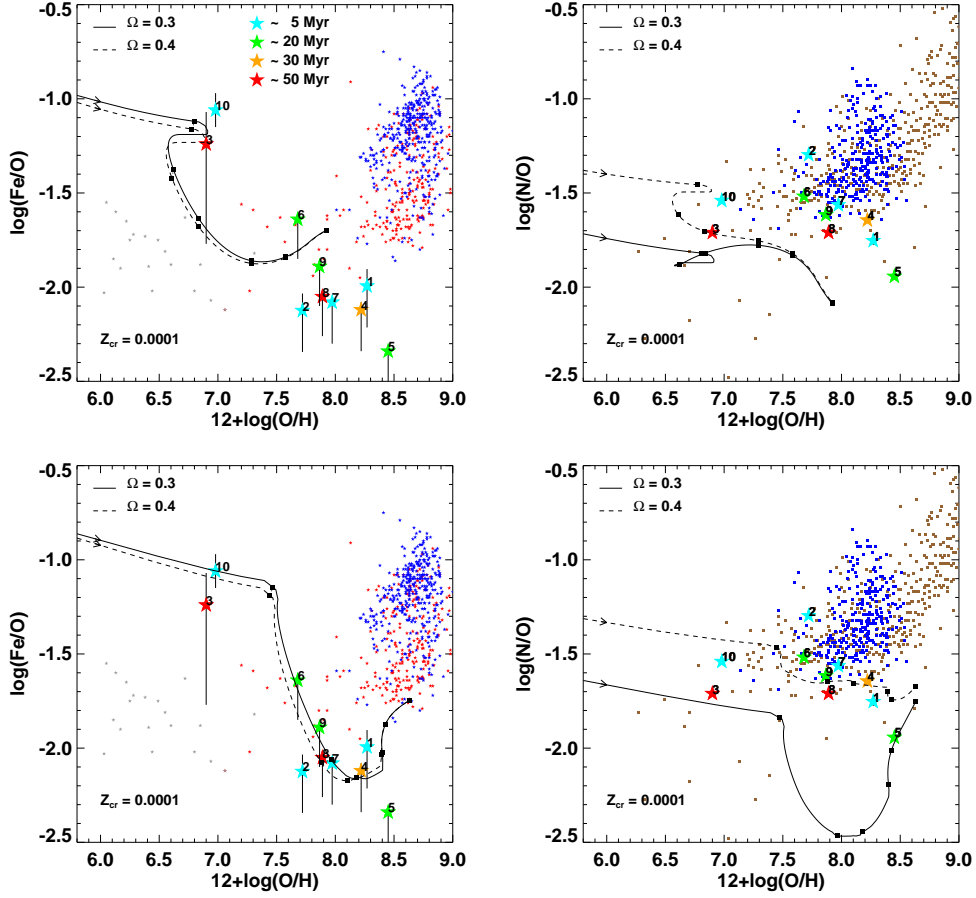
Fig. 2. Comparison of Fe/O (left panels) and N/O (right panels) ratios of EMPGs with predictions from chemical evolution models with yields from rotating PISNs. The upper panels refer to models $M13$ and $M14$ while the lower panels refer to models, $M53$ and $M54$ of Table 1. Large stars, coloured following their estimated ages as shown in the top left panel, are EMPGs from Kojima et al. (2021), from 1-9. Object 10 is from Izotov et al. (2018). In the left panels blue and magenta small stars are thin and thick disc stars respectively (Bensby et al. 2014), while gray small stars are low metallicity stars from Cayrel et al. (2004). In the right panels, small brown squares are local galaxies from Izotov et al. (2006), and blue squares are extragalactic H II regions and high-redshift damped Ly-α systems, assembled from Pettini et al. (2002) Pettini et al. (2008). Solid lines depict the evolution of the abundance ratios of the models in Table 1, in the directions shown by the arrows. The six small black squares along the tracks of the models mark ages at 5, 20, 30 , 60, 100 and 200 Myr, respectively, the latter being larger than the estimated upper limit by Kojima et al. (2021).

6. Later, at an age between 20 and 60 Myr, both models reach the position occupied by the other EMPRESS galaxies. Only EMPG 5 cannot be reproduced by these models, maybe requiring selective dust depletion (Rodríguez & Rubin 2005; Izotov et al. 2006). As far as the N/O ratio is concerned, only model $M54$ is able to fit the observations while model $M53$ has a too low N/O ratio.

3. Conclusions

We have analyzed the peculiarly high Fe/O but normal N/O ratios of very young starburst dominated EMPGs (Kojima et al. 2021). We show that, in order to reproduce the observed high Fe/O ratios observed at 12+log(O/H) ∼ 7, we need to include the effects of PISN from very massive stars. An IMF favouring the formation of massive stars in regions of bursting star formation has been already claimed in the past, and not necessarily in primordial environments (Chiosi et al. 1998; Crowther et al. 2010; Marks et al. 2012; Jeřábková et al. 2018; Zhang et al. 2018; Schneider et al. 2018). We briefly discuss new models of very massive Pop III and very low metallicty stars and confirm that N production from the PISN depends very strongly on the initial degree of rotation, while that of Fe is known to depend much more on the initial mass (Woosley et al. 2002; Takahashi et al. 2018). In our chemical evolution model we assume a threshold metallicity for VMO formation of $Z_{cr} = 0.0001$ and use new yields derived by combining our own rotating PARSEC models with existing explosive models. These models, $M13$ and $M14$ can fit the two EMPGs with the highest Fe/O ratio at the observed metallicity, 12+log(O/H), and the observed young ages (≤ 50 Myr). However, they cannot fit also the other EMPRESS starbursting galaxies that are characterized by a rapid decline of the Fe/O ratio at increasing 12+log(O/H). In this context, we suggest that this other peculiarity could be explained by very high sSFR models producing a fast self-enrichment that first drive the large Fe and O production (large PISN masses) but then, allow only a high O production (lower PISN masses). For this purpose we devise the successful models $M53$ and $M54$ where the late high O production is due to the formation of a small fraction of low mass VMOs obtained by assuming an IMF populated up to $M_i \leq 150$ $M_\odot$ with an exponent $x_{UP} = 0.9$. We remind that similar upper mass limits and upper tail IMF exponents have recently observed in the massive star population in 30 Dor (Schneider et al. 2018). This model could seems quite ad hoc, especially when compared with simulations of the effects of metallicity, dust and UV irradiation on the fragmentation properties of the subsequent stellar generations (Matsukoba et al. 2022; Hirano et al. 2015). But we remind that our goal here is not that of providing a model for the early star formation process. Instead our aim is to show that a suitable combination of PISN can naturally explain both the fast (≤ 50 Myr) and peculiar chemical evolution observed in EMPGs. We also note that there is a mismatch between the age sequence of the models and the observed ages. This could be due to rejuvenation effects caused by multiple intense bursts of star formation that are not sampled by our models. As already discussed in Goswami et al. (2022), if these PISN arise only in high sSFR objects with such a fast evolution, their detection in the local galaxies may be strongly challenged. Finally, we caution that there still exist many uncertainties in single and binary stellar evolution theory that may affect the estimate of masses and metallicities of PISN progenitors, and thus of their yields (e.g. Costa et al. 2021; Di Carlo et al. 2020; Mapelli et al. 2020; Takahashi et al. 2018; Han et al. 2020; Spera et al. 2019; Stanway & Eldridge 2018; Hurley et al. 2002). The study of these galaxies could also be useful to better constrain such uncertainties.

References

Bensby, T., Feltzing, S., & Oey, M. S. 2014, A&A, 562, A71

Bressan, A., Marigo, P., Girardi, L., et al. 2012, MNRAS, 427, 127

Cayrel, R., Depagne, E., Spite, M., et al. 2004, A&A, 416, 1117

Chen, Y., Bressan, A., Girardi, L., et al. 2015, MNRAS, 452, 1068

Chiosi, C., Bressan, A., Portinari, L., & Tantalo, R. 1998, A&A, 339, 355

Costa, G., Bressan, A., Mapelli, M., et al. 2021, MNRAS, 501, 4514

Crowther, P. A., Schnurr, O., Hirschi, R., et al. 2010, MNRAS, 408, 731

Di Carlo, U. N., Mapelli, M., Bouffanais, Y., et al. 2020, MNRAS, 497, 1043

Goswami, S., Silva, L., Bressan, A., et al. 2022, A&A, 663, A1

Goswami, S., Slemer, A., Marigo, P., et al. 2021, A&A, 650, A203

Han, Z.-W., Ge, H.-W., Chen, X.-F., & Chen, H.-L. 2020, Research in Astronomy and Astrophysics, 20, 161

Hirano, S., Hosokawa, T., Yoshida, N., Omukai, K., & Yorke, H. W. 2015, MNRAS, 448, 568

Hirschauer, A. S., Salzer, J. J., Skillman, E. D., et al. 2016, ApJ, 822, 108

Hsyu, T., Cooke, R. J., Prochaska, J. X., & Bolte, M. 2017, ApJ, 845, L22

Hurley, J. R., Tout, C. A., & Pols, O. R. 2002, Monthly Notices of the Royal Astronomical Society, 329, 897

Isobe, Y., Ouchi, M., Kojima, T., et al. 2020, arXiv e-prints, arXiv:2004.11444

Iwamoto, K., Brachwitz, F., Nomoto, K., et al. 1999, ApJS, 125, 439

Izotov, Y. I., Stasińska, G., Meynet, G., Guseva, N. G., & Thuan, T. X. 2006, A&A, 448, 955

Izotov, Y. I. & Thuan, T. X. 1998, ApJ, 500, 188

Izotov, Y. I., Thuan, T. X., & Guseva, N. G. 2012, A&A, 546, A122

Izotov, Y. I., Thuan, T. X., Guseva, N. G., & Liss, S. E. 2018, MNRAS, 473, 1956

Jeřábková, T., Hasani Zonoozi, A., Kroupa, P., et al. 2018, A&A, 620, A39

Kojima, T., Ouchi, M., Rauch, M., et al. 2020, ApJ, 898, 142

Kojima, T., Ouchi, M., Rauch, M., et al. 2021, ApJ, 913, 22

Kozyreva, A., Yoon, S.-C., & Langer, N. 2014, A&A, 566, A146

Limongi, M. & Chieffi, A. 2018, VizieR Online Data Catalog, J/ApJS/237/13

Mapelli, M., Spera, M., Montanari, E., et al. 2020, ApJ, 888, 76

Marks, M., Kroupa, P., Dabringhausen, J., & Pawlowski, M. S. 2012, MNRAS, 422, 2246

Matsukoba, R., Tanaka, K. E. I., Omukai, K., Vorobyov, E. I., & Hosokawa, T. 2022, MNRAS, 515, 5506

Meynet, G., Ekström, S., & Maeder, A. 2006, A&A, 447, 623

Nguyen, C. T., Costa, G., Girardi, L., et al. 2022, A&A, 665, A126

Ohkubo, T., Umeda, H., Maeda, K., et al. 2006, ApJ, 645, 1352

Pettini, M., Ellison, S. L., Bergeron, J., & Petitjean, P. 2002, A&A, 391, 21

Pettini, M., Zych, B. J., Steidel, C. C., & Chaffee, F. H. 2008, MNRAS, 385, 2011

Pustilnik, S. A., Kniazev, A. Y., & Pramskij, A. G. 2005, A&A, 443, 91

Rodríguez, M. & Rubin, R. H. 2005, ApJ, 626, 900

Salvadori, S., Ferrara, A., & Schneider, R. 2008, MNRAS, 386, 348

Schneider, F. R. N., Sana, H., Evans, C. J., et al. 2018, Science, 359, 69

Skillman, E. D., Salzer, J. J., Berg, D. A., et al. 2013, AJ, 146, 3

Spera, M., Mapelli, M., Giacobbo, N., et al. 2019, MNRAS, 485, 889

Stanway, E. R. & Eldridge, J. J. 2018, Monthly Notices of the Royal Astronomical Society, 479, 75–93

Stark, D. P., Ellis, R. S., Charlot, S., et al. 2017, MNRAS, 464, 469

Takahashi, K., Yoshida, T., & Umeda, H. 2018, ApJ, 857, 111

Vanzella, E., Calura, F., Meneghetti, M., et al. 2017, MNRAS, 467, 4304

Volpato, G., Marigo, P., Costa, G., et al. 2022, arXiv e-prints, arXiv:2212.09629

Wise, J. H., Abel, T., Turk, M. J., Norman, M. L., & Smith, B. D. 2012, MNRAS, 427, 311

Woosley, S. E., Heger, A., & Weaver, T. A. 2002, Reviews of Modern Physics, 74, 1015

Yoon, S.-C., Dierks, A., & Langer, N. 2012, A&A, 542, A113

Zhang, Z.-Y., Romano, D., Ivison, R. J., Papadopoulos, P. P., & Matteucci, F. 2018, Nature, 558, 260